

# Geophysical Research Letters

## RESEARCH LETTER

10.1029/2018GL081458

### Key Points:

- A robust streamflow reconstruction is developed for the Chao Phraya River in Thailand using three tree ring oxygen isotope records
- ENSO modulates the Chao Phraya River streamflow, and the level of this modulation is dependent on the ENSO variance
- The number of high-flow events increases during La Niña events, and such increases fluctuate at a decadal timescale

### Supporting Information:

- Supporting Information S1

### Correspondence to:

C. Xu,  
cxxu@mail.jggcas.ac.cn

### Citation:

Xu, C., Buckley, B. M., Promchote, P., Wang, S.-Y. S., Pumijumnong, N., An, W., et al. (2019). Increased variability of Thailand's Chao Phraya River peak season flow and its association with ENSO variability: Evidence from tree ring  $\delta^{18}\text{O}$ . *Geophysical Research Letters*, 46, 4863–4872. <https://doi.org/10.1029/2018GL081458>







Received 1 DEC 2018

Accepted 2 APR 2019

Accepted article online 18 APR 2019

Published online 3 MAY 2019

## Increased Variability of Thailand's Chao Phraya River Peak Season Flow and Its Association With ENSO Variability: Evidence From Tree Ring $\delta^{18}\text{O}$

Chenxi Xu<sup>1,2</sup> , Brendan M. Buckley<sup>3</sup> , Parichart Promchote<sup>4</sup> , S.-Y. Simon Wang<sup>4</sup> , Nathsuda Pumijumnong<sup>5</sup>, Wenling An<sup>1,2</sup>, Masaki Sano<sup>6</sup> , Takeshi Nakatsuka<sup>7</sup>, and Zhengtang Guo<sup>1,2,8</sup> 

<sup>1</sup>Key Laboratory of Cenozoic Geology and Environment, Institute of Geology and Geophysics, Chinese Academy of Sciences, Beijing, China, <sup>2</sup>CAS Center for Excellence in Life and Paleoenvironment, Beijing, China, <sup>3</sup>Tree Ring Lab, Lamont-Doherty Earth Observatory, Columbia University, Palisades, NY, United States, <sup>4</sup>Department of Plants, Soils, and Climate, Utah State University, Logan, UT, USA, <sup>5</sup>Faculty of Environment and Resource Studies, Mahidol University, Nakhon Pathom, Thailand, <sup>6</sup>Research Institute for Humanity and Nature, Kyoto, Japan, <sup>7</sup>Faculty of Human Sciences, Waseda University, Tokorozawa, Japan, <sup>8</sup>University of Chinese Academy of Sciences, Beijing, China

**Abstract** We present a statistically robust reconstruction of Thailand's Chao Phraya River peak season streamflow (CPRPF) that spans the 202 years from 1804 to 2005 CE. Our reconstruction is based on tree ring  $\delta^{18}\text{O}$  series derived from three *Pinus merkusii* sites from Laos and Thailand. The regional  $\delta^{18}\text{O}$  index accounts for 57% of the observed variance of CPRPF. Spatial correlation and 21-year running correlation analyses reveal that CPRPF is greatly influenced by regional precipitation variations associated with the El Niño–Southern Oscillation (ENSO). Periods of enhanced and reduced ENSO activity are associated with strong and weak ENSO–streamflow correlation, respectively. At the longer timescale, the Pacific Decadal Oscillation (PDO) appears to modulate the ENSO–streamflow correlations, with the most extreme flood events along the Chao Phraya River occurring during periods of increased frequency of La Niña events that coincide with extended cold phases of the PDO. The CPRPF reconstruction could aid management planning for Thailand's water resources.

**Plain Language Summary** We present a 202-year reconstructed record of the peak season streamflow from the Chao Phraya River in Thailand. Our reconstruction is derived from the average of  $\delta^{18}\text{O}$  from three tree ring sites in Thailand and Laos, upstream of the Chao Phraya River. We found strong connection between the streamflow and the Pacific Ocean climate modes. The result reveals short-term pulses in extreme flow conditions embedded in the longer-term climate variations. Such information could be used to assess streamflow variation and thereby aid water management planning.

## 1. Introduction

The Chao Phraya River (CPR) Basin encompasses one third of Thailand's total area, comprised of the country's four major rivers that drain the north (Ping and Wang) and east (Yom and Nan) regions of the country (Figure 1a). Being the largest river basin in Thailand, changes in the CPR flow regime have a direct impact on Thailand's agricultural and economic sectors (Siripong et al., 2000). Severe flooding in 1995 and 2011 caused billions of dollars in damage (Promchote et al., 2016; Re, 2011; Siripong et al., 2000). Given its importance, it is imperative to understand the processes that control CPR peak flow (CPRPF) and evaluate the implications of future changes to the regional climate. Despite marked uncertainty, the mean annual river discharge for the CPR basin is projected to increase (Kure & Tebakari, 2012), while discharge for the small tributaries of the CPR may decrease (Hunukumbura & Tachikawa, 2012). The instrumental streamflow record of CPR extends only as far as 1956, however, which is an insufficient timespan to capture long-term changes of flow related to multidecadal to centennial climate variability. Proxy reconstructions of the magnitude, intensity, and periodicity of streamflow variations at different time scales will therefore be of value for determining the primary factors that control CPRPF.

One promising way to extend the instrumental record of streamflow is to utilize regional tree ring records as proxies for streamflow through the connection to hydroclimate (e.g., Stockton & Jacoby, 1976). Due to their annual resolution, tree rings are easily comparable with observed streamflow data and have been

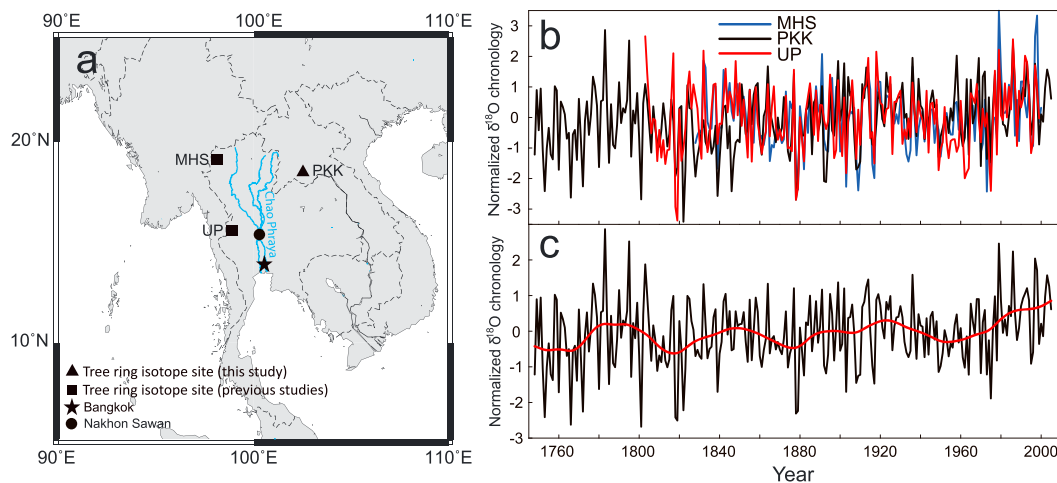


**Figure 1.** Map of the study area showing (a) the locations of the three *Pinus merkusii* sites used for this study (black squares and triangle), along with the Nakhon Sawan gauging station (black circle) on the Chao Phraya River and tributaries (blue lines). In (b) we plot the three  $\delta^{18}\text{O}$  series used for this study along with in (c) the composite regional  $\delta^{18}\text{O}$  record for 1748–2005. The red line (30-year splined values) emphasizes the decadal variability of changes in  $\delta^{18}\text{O}$  over the past 257 years.

successfully applied in many regions of the world for reconstructing streamflow (e.g., D'Arrigo et al., 2011; Deroose et al., 2015; Gou et al., 2010; Lara et al., 2008; Meko et al., 2012; Nguyen & Galelli, 2017; Woodhouse et al., 2006). Despite the challenges associated with cross-dating tropical tree rings, a growing body of annually dated tree ring records have emerged from Southeast Asia that make it possible to attempt such a reconstruction for the CPR. Previous tree ring studies from the CPR basin include research on two *Pinus* species (*P. merkusii* and *P. kesiya*), and it is a selection of these records that form the basis of the current study (Buckley et al., 1995, 2005, 2007; D'Arrigo et al., 1997; Pumijumong & Eckstein, 2011). However, prior studies reveal that annual ring width measurements from these two Pines from Laos and Thailand do not significantly correlate with monsoon season precipitation but rather yield a less easily interpretable relationship with regional climate (e.g., Buckley et al., 1995, 2005, 2007; D'Arrigo et al., 1997; Pumijumong & Eckstein, 2011). As a result, we do not utilize the ring width records from our pine sites as predictors of CPRPF, relying instead on the stable isotope records as discussed below.

Recent studies of  $\delta^{18}\text{O}$  from the cellulose of Southeast Asian tree species have demonstrated a connection to regional hydroclimate variability with unprecedented clarity (Sano et al., 2012; Xu, Pumijumong, et al., 2018; Xu et al., 2015; Xu et al., 2011; Xu, Sano, et al., 2013; Zhu, Stott, Buckley, & Yoshimura, 2012; Zhu, Stott, Buckley, Yoshimura, & Ra, 2012). These studies all showed that tree ring  $\delta^{18}\text{O}$  is significantly correlated with monsoon season precipitation (Xu et al., 2015; Xu, Sano, et al., 2013; Zhu, Stott, Buckley, & Yoshimura, 2012; Zhu, Stott, Buckley, Yoshimura, & Ra, 2012). In addition, Xu et al. (2015) found no age-related effect on tree ring  $\delta^{18}\text{O}$  for *Pinus merkusii* in Thailand. Therefore, regional tree ring  $\delta^{18}\text{O}$  should be applicable to reconstructing streamflow with little loss of low-frequency variability, as is often the case with ring width-based reconstructions of climate. While tree ring width is limited in its ability to capture peak flow due to ecophysiological factors related to the law of limiting factors (Fritts, 1976),  $\delta^{18}\text{O}$  as a geochemical measurement is not necessarily constrained by the same ecophysiological factors.

For this study we developed a regional *Pinus merkusii*  $\delta^{18}\text{O}$  index for the CPRB based on the average of three tree ring  $\delta^{18}\text{O}$  time series in northern and central Thailand, and northcentral Laos (MHS, UP, and PKK, respectively, as shown in Figure 1a). The PKK  $\delta^{18}\text{O}$  time series from Laos is presented for the first time here, along with two previously published records from Thailand ( $\delta^{18}\text{O}$  in UP from Xu, Pumijumong, et al., 2018, and  $\delta^{18}\text{O}$  in MHS from Xu et al., 2015).

## 2. Materials and Methods

### 2.1. *Pinus merkusii* $\delta^{18}\text{O}$ Chronology Development in Northcentral Laos

With this study we present the first  $\delta^{18}\text{O}$  time series from crossdated *Pinus merkusii* cores from the Phou Khao Khouay National Biodiversity Conservation area (PKK) in northcentral Laos (Figure 1a). These trees

were collected, crossdated, and measured for ring width by Buckley et al. (2007). These authors determined that while direct correlation with rainfall and temperature were weakly expressed, the most significant correlations were found between ring width and tropical Pacific sea surface temperatures (SSTs) along the regions associated with El Niño–Southern Oscillation (ENSO). From the Buckley et al. (2007) core collection we selected five trees for stable isotope analyses (ANMPM06, ANMPM09, ANMPM13, ANMPM14, and TGLPM04), choosing samples that exhibited the fewest missing rings and the highest correlation with the master chronology. These samples were accurately crossdated, and all information on the study area, cross-dating procedures, and the climatic implications of ring width in PKK can be found in Buckley et al. (2007). We used the modified plate method to extract  $\alpha$ -cellulose from wood plate samples as described by Xu et al. (2011) and Xu, Zheng, et al. (2013). Oxygen isotope ( $\delta^{18}\text{O}$ ) measurements from the tree ring samples were determined by an isotope ratio mass (Delta V Advantage, Thermo Scientific) at the Research Institute for Humanity and Nature, Japan. The analytical uncertainty for repeated measurements of cellulose was approximately  $\pm 0.19\text{‰}$  ( $n = 115$ ).

The mean values of the  $\delta^{18}\text{O}$  time series from the five selected core samples (ANMPM06, ANMPM09, ANMPM13, ANMPM14, and TGLPM04 as shown in Figure S1a) are 23.52‰, 23.58‰, 23.54‰, 22.80‰, and 24.27‰, respectively, during the common period of 1868–1995. The corresponding standard deviations for each series are 1.17‰, 0.91‰, 1.17‰, 1.00‰, and 1.24‰. The yearly  $\delta^{18}\text{O}$  standard deviations for the five trees vary between 0.21‰ and 1.61‰ (mean = 0.77‰). Intertree  $\delta^{18}\text{O}$  variations show high coherence (Table S1 and Figure S1 in the supporting information), reflecting their common response to climate. All five tree ring  $\delta^{18}\text{O}$  time series were normalized based on the common period of 1868–1995 and were then averaged to produce the PKK  $\delta^{18}\text{O}$  index (Figure S1c). The first order autocorrelation for PKK  $\delta^{18}\text{O}$  is 0.20, which is similar with the two other *Pinus merkusii*  $\delta^{18}\text{O}$  indices used for this study: from MHS (0.17, Xu et al., 2015) and UP (0.16, Xu, Pumijumnong, et al., 2018). The low autocorrelation for all three  $\delta^{18}\text{O}$  records indicates that physiological processes from prior years are not significantly correlated with  $\delta^{18}\text{O}$  values in any given year, something that is often strongly expressed for ring width time series (Fritts, 1976). All three  $\delta^{18}\text{O}$  records are significantly correlated with the monsoon season precipitation in the CPR basin and were therefore combined to reconstruct the CPRPF for the past 257 years.

## 2.2. Regional $\delta^{18}\text{O}$ Chronology Development

The three *Pinus merkusii*  $\delta^{18}\text{O}$  records used for the current study include MHS from northwestern Thailand (Xu et al., 2015), and UP from westcentral Thailand (Xu, Pumijumnong, et al., 2018), in addition to PKK from central Laos included here for the first time. These records are significantly correlated with the monsoon season precipitation in the CPR basin (Figure S2) and were subsequently combined for use in reconstructing peak monsoon rainfall, passing all of the rigorous statistical tests for calibration and verification commonly employed in dendroclimatology. The three tree ring  $\delta^{18}\text{O}$  records are also significantly correlated with each other as shown in Figure 1b ( $r_{\text{PKK-UP}} = 0.46$ ;  $r_{\text{PKK-MHS}} = 0.53$ ; and  $r_{\text{MHS-UP}} = 0.60$ ), reflecting a common forcing from the regional monsoon season precipitation. We therefore normalized all three records over the common period of 1828–1999 and took their average to produce a regional  $\delta^{18}\text{O}$  index (CPRB18O as plotted in Figure 1c).

## 2.3. Climatic and Statistical Analyses

To explore the streamflow relationship with climate variations, we compared our record against several climatic indices: Niño 3.4 from National Oceanic and Atmospheric Administration (NOAA) Climate Prediction Center, Pacific Decadal Oscillation (PDO) index from Mantua et al. (1997), Indian Ocean dipole index from Saji et al. (1999), and regional gridded precipitation and global SST data sets from the NOAA/Office of Oceanic and Atmospheric Research (OAR)/Earth System Research Laboratory (ESRL) Physical Sciences Division (PSD). Precipitation data from CRU TS4.0 and SST from the COBE-SST2 data set, also provided by the NOAA/OAR/ESRL PSD, were used to evaluate the spatial correlation and regression between the  $\delta^{18}\text{O}$  series/observed streamflow of the CPR and regional precipitation/SST. In addition, six tropical Pacific SST reconstructions (Cook et al., 2008; Emile-geay et al., 2013; Li et al., 2013; Liu et al., 2017; McGregor et al., 2010; Tierney et al., 2015) were averaged to produce a composite ENSO index, which

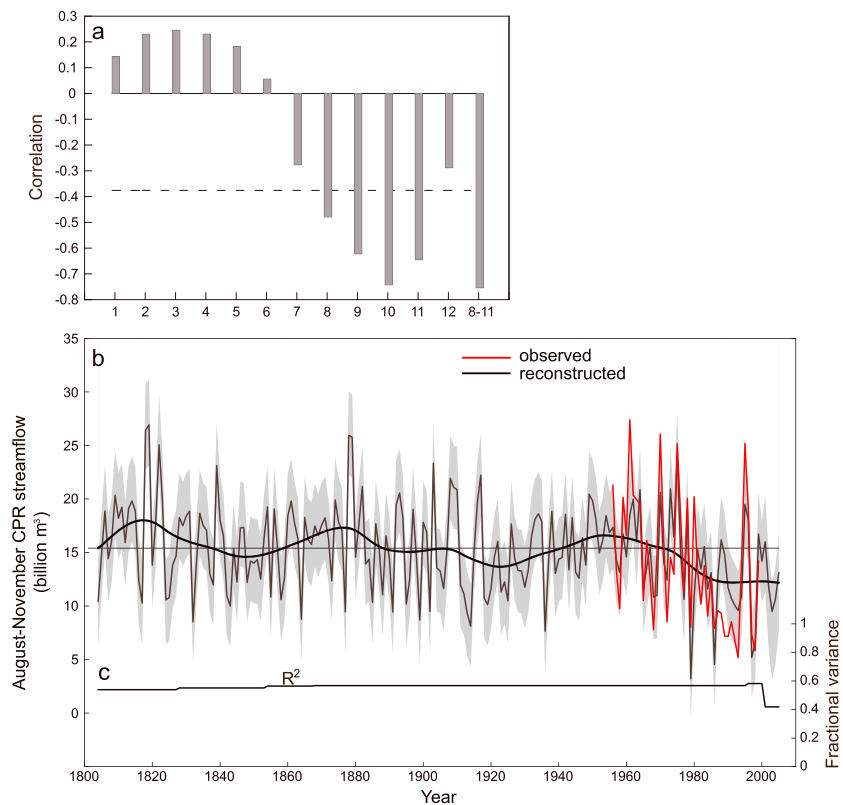


**Figure 2.** The top panel (a) plots the correlation coefficients between monthly Chao Phraya River (CPR) streamflow and the CPRB180 index for the period of 1956–1999. The dashed line shows the 95% confidence limit, exceeded by months 8–11 (August–November). In the middle panel (b) we plot the full 1804–2005 Chao Phraya River peak season (August–November) flow reconstruction with the standard error of uncertainty shown by the gray shading around the mean. The red line in (b) is the observed values against the reconstructed values in black with decadal variability shown by the heavy black line (30-year splined values). In the bottom panel (c) we plot the time-varying calibration and verification statistics over the period 1804–2005.

was then used to explore the impact of remote oceans on CPRPF. Two PDO reconstructions (MacDonald & Case, 2005; Shen et al., 2006) were averaged as a composite index to evaluate PDO's modulation on CPRPF.

### 3. Results and Discussion

While evaluating the relationship between the CPR streamflow and tree ring  $\delta^{18}\text{O}$ , we found that the peak flow coincides with the summer monsoon precipitation during the August–November period, which accounts for 63% of the annual discharge. Based on these relationships, we followed the methodology described by Cook and Kairiukstis (1990) and employed a linear regression model to transfer the tree ring  $\delta^{18}\text{O}$  data to CPRPF in order to produce a statistically robust reconstruction of peak season streamflow. The Pearson's correlation coefficient ( $r$ ), explained variance ( $R^2$ ), reduction of error, and coefficient of efficiency (CE) were used to evaluate the validity of the linear regression model (Cook et al., 1999) and are shown in Table S2.

#### 3.1. Climate Response of CPRB180 and Streamflow

We conducted correlation analyses between CPRB180 and CPR monthly streamflow from the Nakhon Sawan gauging station and reveal a significant, negative correlation ( $-0.76$  during the common period of 1956–1999,  $p < 0.01$ ) between CPRB180 and August–November streamflow. This is consistent with the anticorrelation between rainfall amount and  $\delta^{18}\text{O}$  known as the “amount effect” (Risi et al., 2008). A similar negative correlation between tree ring  $\delta^{18}\text{O}$  and streamflow was also found for northern Lao cypress and northern Thailand *P. merkusii* (Xu et al., 2015; Xu, Sano, et al., 2013, respectively).

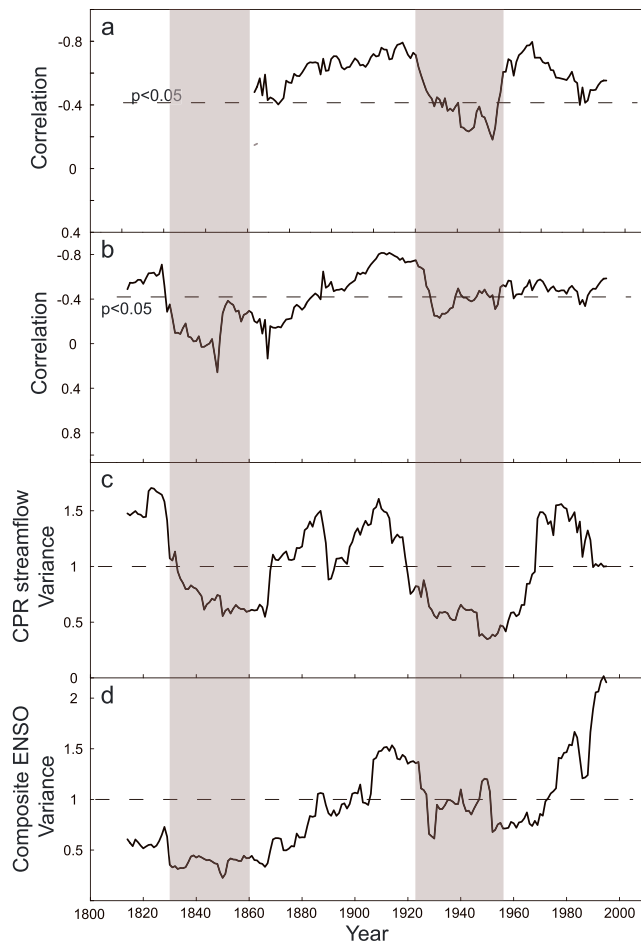


**Figure 3.** Twenty-one-year running correlations between our reconstructed Chao Phraya River (CPR) streamflow and the observed Niño 3.4 Index (a), and the Composite El Niño–Southern Oscillation (ENSO) index (b) (the gray dashed lines in panels (a) and (b) indicate the 95% confidence levels). In panels (c) and (d) we plot the 21-year running variance for CPR streamflow and composite ENSO index, respectively.

21-year running variance of CPRPF showed reduced variance in the period of 1830–1860 and 1920–1960 (Figure 3c).

### 3.2. Human Impacts on CPRPF

The Chao Phraya River has undergone considerable human modifications (Siripong et al., 2000), exemplified by the construction of Bhumibol Dam and Sirikit dam in 1968 and 1972, respectively. These dams combined control 22% of the Chao Phraya's annual runoff. Shifting cultivation and irrigation also changed the hydrological regime (Siripong et al., 2000). To gauge the possible influence of human activity on CPRPF at Nakhon Sawan, we calculated the spatial correlation of May–October precipitation in the upper and middle reaches of the CPR and subsequently found significant positive correlations ( $r = 0.83$ ,  $p < 0.0001$ ) with the observed CPRPF (Figure S4a). Moreover, the 21-year running correlation between observed CPRPF and May–October precipitation is relatively stable during the last 50 years ( $r > 0.78$ ; Figure S4b). These results indicate that the sheer volume of the rainy season precipitation profoundly influences CPRPF at Nakhon Sawan, despite the increased intervention of streamflow by human activities. Nevertheless, human activities (i.e., damming) inevitably would lead to certain degrees of uncertainty in the river flow itself, and this uncertainty would be added on top of the regression model's uncertainty, which is shown in Figure 2b in the form of plus/minus standard error (bottom of the graph), following Esper et al. (2007).

There are very few statistically calibrated and verified reconstructions of streamflow from tropical Asia. D'Arrigo et al. (2011) reconstructed Indonesia's Citarum River based on ring width measurements from regional teak sites that exhibited a strong direct correlation between rainfall and September–November streamflow. More recently, Nguyen and Galelli (2017) used the tree ring width-derived Monsoon Asia Drought Atlas data (Cook et al., 2010) to reconstruct the annual flow of north Thailand's Ping River. In comparison, our simple linear regression using the CPRB18O as a predictor resulted in a reconstruction model that accounted for 57% of the variation in CPRPF for the period 1956–1999. In our model, both reduction of error and CE statistics were well above 0 during the period of 1804–1999, indicating a predictive skill that satisfies common calibration and verification measures (Table S2). However, due to low sample depth, our reconstruction is not robust prior to 1804 and after 2000, as indicated by the CE statistic (Table S2), a metric that is affected by low sample depth (Cook & Kairiukstis, 1990). Despite the increased difference between the reconstructed and observed CPRPF during the period of 1987–1992, which may be related to the reduced variance of observed CPRPF, the reconstructed and observed CPRPF show consistent variations during most of the common period (Figure 2b). Because our CPRPF reconstruction prior to 1804 is based on only two tree ring  $\delta^{18}\text{O}$  series from central Laos and the CE values are below zero during the period of 1748–1803 (Table S2 and Figure S1), all ensuing analyses of our CPRPF reconstruction focuses on the robust period of our reconstruction since 1804.

We used one standard deviation from the mean as a threshold for determining extreme drought and flood events for CPRPF and reveal a history of extreme high and low flows of the CPR from 1804 to 2005 (Figure 2b). The full reconstruction mean and standard deviation ( $\sigma$ ) are 15.25 and  $4.13 \times 10^9 \text{ m}^3$ , respectively. Spectral analyses based on the multitaper method (Mann & Lees, 1996) indicate that CPRPF contains interannual (2–7 years) and multidecadal (~67 years) variations at a confidence level greater than 95% (Figure S3). A 21-year running average highlights the decadal-scale fluctuations, with high streamflow periods ( $>1\sigma$ ) for 1804–1830, 1860–1885, and 1940–1970 and low flow periods for 1900–1940 and 1971–2000 (Figure 2b). The



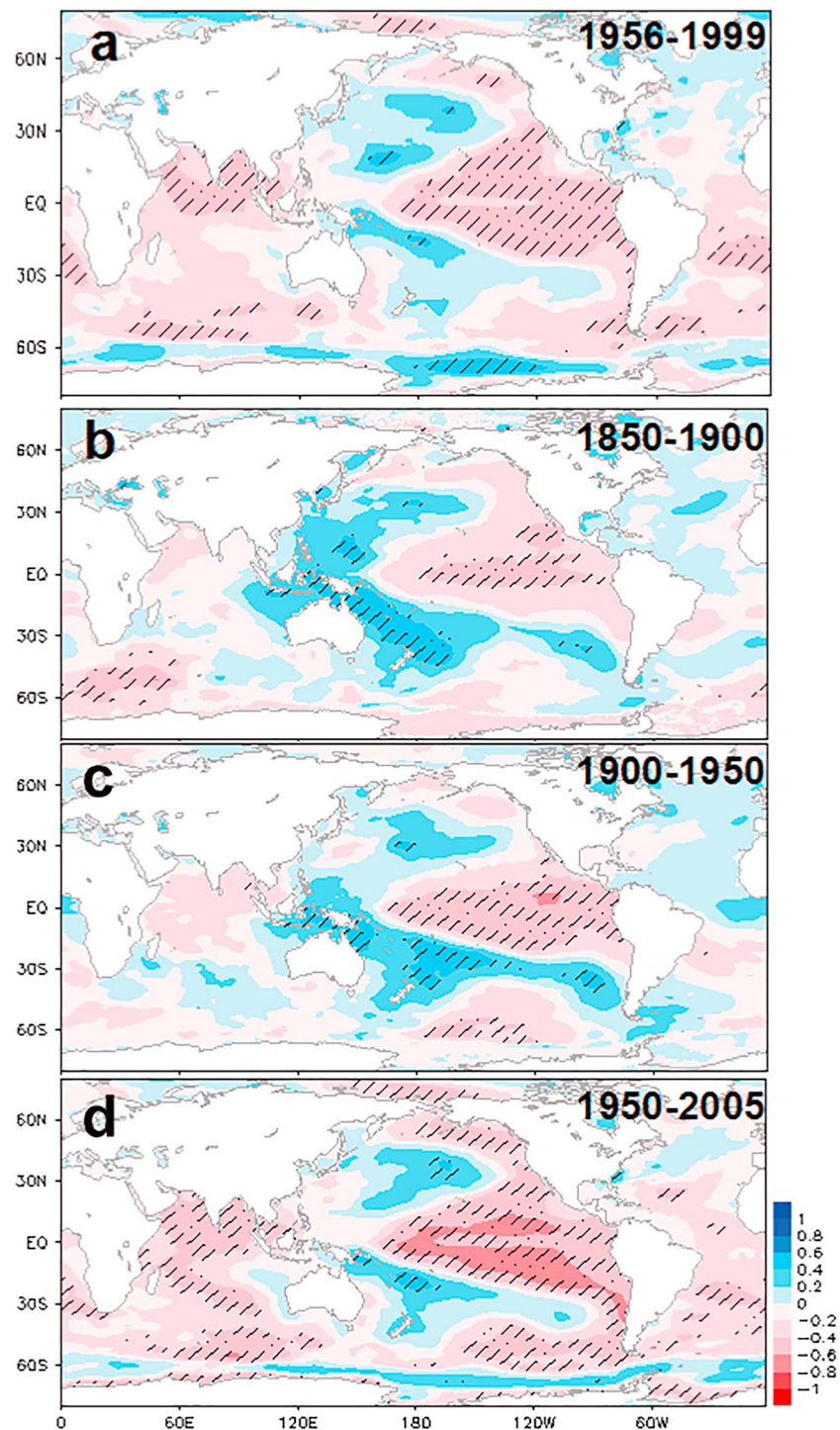


**Figure 4.** Correlation patterns of sea surface temperature (May–December) with (a) observed streamflow (August–November, 1956–1999) and (b–d) reconstructed streamflow for three periods (August–November, 1850–1900, 1900–1950, 1950–2005, respectively). Hatched areas indicate the significance of correlation coefficients that exceed the 99% level of confidence.

### 3.3. Climate Influences on CPRPF Variations From Remote Oceans

The observed CPRPF correlates significantly ( $p < 0.05$ ) with the May–December Niño 3.4 index and July–December PDO index over the period of 1956–1999 (Table S2). The sliding correlation analysis

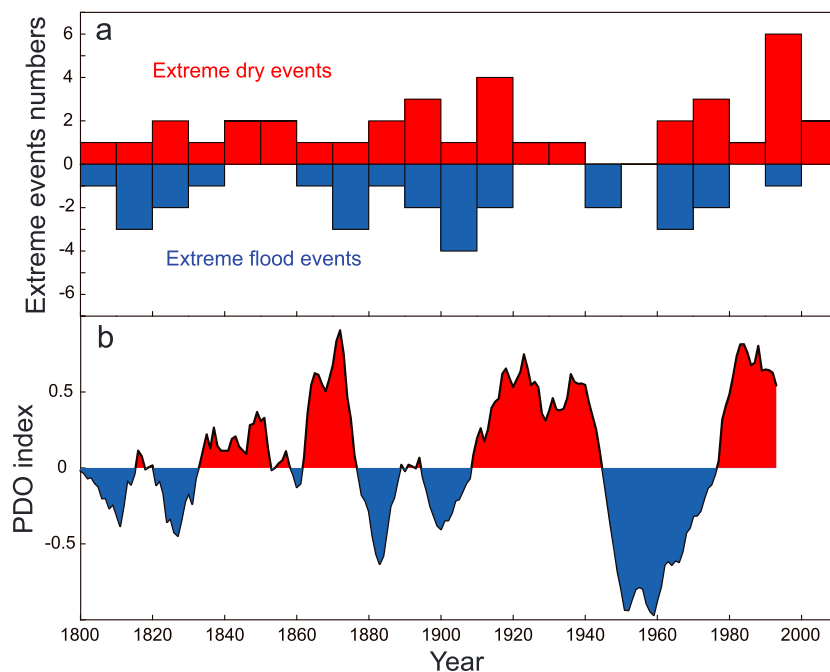


**Figure 5.** In (a) we plot the number of extreme drought (red bars) and flood events (blue bars) per decade, as derived from our Chao Phraya River peak-season streamflow reconstruction; in (b) we plot the 11-year running average of the composite Pacific Decadal Oscillation (PDO) index during the last two hundred years with red reflecting positive PDO and blue negative PDO.

between ENSO and our reconstructed CPRPF shows generally strong correspondence for the period 1854–2005, but weakening between 1921–1960 and 1831–1860 when the CPRPF and ENSO variances were both low (Torrence & Webster, 1999, Figures 3a, 3c, and 3d). The observed CPRPF is positively correlated over the entire CPR basin (Figure S4), which suggests a regional-scale response to ENSO that is consistent with previous studies (D'Arrigo et al., 2011; Liu et al., 2011; Xu et al., 2016; Xu, Shi, et al., 2018; Xu, Zheng, et al., 2013). Specifically, Xu, Pumijumnong, et al. (2018) showed that ENSO affects the rainy season precipitation in the central part of the CPR basin and suggested that the reduction in the ENSO-precipitation relationship between 1930 and 1970 corresponds to the reduced ENSO variance. We computed the spatial correlation map between the observed CPRPF and May–December SST, and the result in Figure 4a outlines a warm-phase ENSO (El Niño) with warmer water over the central-eastern Pacific and the northern Indian Ocean. However, the ENSO-precipitation relationship in the upper CPR basin dissipated during the last 20 years and earlier studies have suggested that this phenomenon may be related to the shift of the descending arm of the Walker Circulation (Singhrattana et al., 2005; Xu et al., 2015).

In order to examine the interdecadal changes in the streamflow-ENSO relationship as inferred from Figure 3, we computed the SST correlation maps with the reconstructed streamflow for three different periods, 1850–1900, 1900–1950, and 1950–2005 (Figures 4–4d, respectively). Based on the relationship between observed CPRPF and ENSO/PDO (Table S3), May–December SST across the Pacific has the strongest influences on streamflow and was therefore used for all correlation maps. The results are consistent with a warming over the central-eastern Pacific associated with varying SST patterns elsewhere (Figure 4). Some features are noteworthy, including the more recent appearance of the northern Indian Ocean correspondence (Figure 4d) and the relatively strong western tropical Pacific and the western South Pacific signals during the earlier period (Figures 4b and 4c). We also observed a change in the classic “horseshoe” shape of the PDO in the central North Pacific and the eastern-Pacific coast during the recent period of 1950–2005 (Zhang & Delworth, 2015), which coincides with the more robust ENSO pattern and its possible increase in teleconnection effects over Southeast Asia (Li et al., 2018; Stuecker, 2018; Yu et al., 2010, 2012). Furthermore, the recent intensification of the northern Indian Ocean connection (Figure 4d) seems indicative of the monsoon forcing in modulating the CPRPF. These results further support the

changing ENSO pattern and the increase of ENSO variances as shown in Figure 4d. We should note that while the spatial correlations (Figure 4) also seems to depict the Interdecadal Pacific Oscillation (IPO) pattern (Dong & Dai, 2015; Meehl et al., 2013), a comparison of our CPRPF reconstruction with a new IPO reconstruction (Buckley et al., 2019) reveals that the present CPRPF reconstruction is not significantly correlated with the IPO.

During El Niño, Southeast Asian droughts may increase in intensity, especially so during PDO warm phases (Wang et al., 2014). When the PDO is in phase with ENSO, their combined impact on precipitation and CPRPF may be enhanced by the SST gradient across the central-western Pacific (Figure 4d, 1950–2005). Such intensification might also be expected to strengthen the monsoon trough over the CPRB. By highlighting the protracted, extreme drought and flood events in Figure 5 (1810–1830, 1900–1920, and 1960–1980), a marked increase is revealed over the last two decades. Based on the comparison between an 11-year running average of the composited PDO index and extreme events for CPRPF (Figure 5), the number of extreme flood events appears to increase when PDO is in its cold phase (e.g., 1960–1980) and decrease when PDO is in its warm phase (e.g., 1920–1940 and 1980–2000). The post-1980 warm phases of PDO correspond to the increase in extreme drought as expressed by reduced CPRPF. Similar relationships between monsoon rainfall and PDO were also reported over India and Myanmar (Roy et al., 2003; Sen Roy & Sen Roy, 2011). All of these results indicate that PDO may be the most important factor modulating the interdecadal variability of extreme events for CPRPF.

#### 4. Conclusions

A regional tree ring cellulose  $\delta^{18}\text{O}$  (CPRB18O) record was developed from the Chao Phraya River basin in Thailand for the period 1804–2005, based on the combination of three  $^{18}\text{O}$  tree ring records from Thailand and Laos. The CPRB18O chronology is significantly, negatively correlated ( $r = -0.76$ ,  $p < 0.01$ ) with the August–November CPR streamflow, allowing for a robust reconstruction (57% explained variance) of peak flow for the past 202 years. Our reconstruction reveals significant interannual variability within 2–7 years that is coincident with the influence of ENSO. This association is corroborated by statistically significant correlation with several ENSO data sets. The CPRPF-ENSO relationship appears to be influenced by the change in ENSO variance, such that periods of enhanced or reduced ENSO activity are associated with strong or weak ENSO-CPRPF correlation, respectively. Different phases of the PDO also appear to modulate the ENSO-CPRPF relationship, in that the number of extreme flood events increased during ENSO cool phase (La Niña) and more so during the PDO cold phase. Combined with projected increases in ENSO variance (Cai et al., 2014; Yoon et al., 2015), the CPRPF reconstruction presented here could implicate a more fluctuating future when it comes to extreme events.

#### References

- Buckley, B. M., Barbetti, M., Watanasak, M., D'Arrigo, R. D., Boonchirdchoo, S., & Sarutanon, S. (1995). Dendrochronological investigations in Thailand. *IAWA Journal*, 16(4), 393–409. <https://doi.org/10.1163/22941932-90001429>
- Buckley, B. M., Cook, B. I., Bhattacharyya, A., Dukpa, D., & Chaudhary, V. (2005). Global surface temperature signals in pine ring-width chronologies from southern monsoon Asia. *Geophysical Research Letters*, 32, L20704. <https://doi.org/10.1029/2005GL023745>
- Buckley, B. M., Duangsathaporn, K., Palakit, K., Butler, S., Syhapanya, V., & Xaybouangeun, N. (2007). Analyses of growth rings of *Pinus merkusii* from Lao PDR. *Forest Ecology and Management*, 253(1–3), 120–127. <https://doi.org/10.1016/j.foreco.2007.07.018>
- Buckley, B. M., Ummenhofer, C. C., D'Arrigo, R. D., Hansen, K. G., Truong, L. H., Le, C. N., & Stahle, D. K. (2019). Interdecadal Pacific Oscillation reconstructed from trans-Pacific tree rings: 1350–2004 CE. *Climate Dynamics*. <https://doi.org/10.1007/s00382-019-04694-4>
- Cai, W., Borlace, S., Lengaigne, M., Van Rensch, P., Collins, M., Vecchi, G., & England, M. (2014). Increasing frequency of extreme El Niño events due to greenhouse warming. *Nature Climate Change*, 4(2), 111–116. <https://doi.org/10.1038/nclimate2100>
- Cook, E., Anchukaitis, K., Buckley, B. M., D'Arrigo, R., Jacoby, G., & Wright, W. (2010). Global monsoon failure and megadrought during the last millennium. *Science*, 328(5977), 486–489. <https://doi.org/10.1126/science.1185188>
- Cook, E., & Kairiukstis, L. (1990). *Methods of dendrochronology*. Netherlands: Kluwer.
- Cook, E., Meko, D., Stahle, D., & Cleaveland, M. (1999). Drought reconstructions for the continental United States. *Journal of Climate*, 12(4), 1145–1162. [https://doi.org/10.1175/1520-0442\(1999\)012<1145:DRFTCU>2.0.CO;2](https://doi.org/10.1175/1520-0442(1999)012<1145:DRFTCU>2.0.CO;2)
- Cook, E. R., D'Arrigo, R. D., and K. Anchukaitis (2008) ENSO reconstructions from long tree-ring chronologies: Unifying the differences, in: Talk presented at a special workshop on Reconciling ENSO Chronologies for the Past 500 Years, held in Moorea, French Polynesia on 2–3 April 2008, 2008.
- D'Arrigo, R., Abram, N., Ummenhofer, C., Palmer, J., & Mudelsee, M. (2011). Reconstructed streamflow for Citarum River, Java, Indonesia: Linkages to tropical climate dynamics. *Climate Dynamics*, 36(3–4), 451–462. <https://doi.org/10.1007/s00382-009-0717-2>
- D'Arrigo, R., Barbetti, M., Watanasak, M., Buckley, B. M., Krusic, P., & Sarutanon, S. (1997). Progress in dendroclimatic studies of mountain pine in northern Thailand. *IAWA Journal*, 18(4), 433–444. <https://doi.org/10.1163/22941932-90001508>

#### Acknowledgments

We are most grateful for the helpful comments by the Editor and two anonymous reviewers that greatly improved our manuscript. This study is supported by the Strategic Priority Research Program of the Chinese Academy of Sciences, grants XDB26020000 and XDA13010106, the National Natural Science Foundation of China, grants 41672179, 41671193, 41630529, 41430531, 41690114, and 41888101, the Chinese Academy of Sciences (CAS) Pioneer Hundred Talents Program, and the National Key R&D Program of China, grants 2016YFA0600502 and 2017YFE0112800. B. M. Buckley was supported by funding from the US National Science Foundation (AGS 13-03976 and AGS 16-02629) and the Lamont-Doherty Earth Observatory's Climate Center and Center for Climate and Life. This is Lamont contribution 8314. The tree ring-based streamflow reconstruction data in this study are available from the NOAA Paleoclimatology Datasets (<https://www.ncdc.noaa.gov/paleo/study/26610>).



- Derose, R., Bekker, M., Wang, S., Buckley, B. M., Kjelgren, R., Bardsley, T., et al. (2015). A millennium-length reconstruction of Bear River streamflow, Utah. *Journal of Hydrology*, 529, 524–534. <https://doi.org/10.1016/j.jhydrol.2015.01.014>
- Dong, B., & Dai, A. (2015). The influence of the interdecadal Pacific oscillation on temperature and precipitation over the globe. *Climate Dynamics*, 45(9–10), 2667–2681. <https://doi.org/10.1007/s00382-015-2500-x>
- Emile-geay, J., Cobb, K., Mann, M., & Wittenberg, A. (2013). Estimating central equatorial Pacific SST variability over the past millennium. Part I: Methodology and validation. *Journal of Climate*, 26(7), 2329–2352. <https://doi.org/10.1175/JCLI-D-11-00511.1>
- Esper, J., Frank, D., Büntgen, U., Verstege, A., Luterbacher, J., & Xoplaki, E. (2007). Long-term drought severity variations in Morocco. *Geophysical Research Letters*, 34, L17702. <https://doi.org/10.1029/2007GL030844>
- Fritts, H. C. (1976). *Tree Rings and Climate*. London, New York, San Francisco: Academic Press.
- Gou, X., Deng, Y., Chen, F., Yang, M., & Fang, K. (2010). Tree ring based streamflow reconstruction for the Upper Yellow River over the past 1234 years. *Chinese Science Bulletin*, 55(36), 4179–4186. <https://doi.org/10.1007/s11434-010-4215-z>
- Hunukumbura, P., & Tachikawa, Y. (2012). River discharge projection under climate change in the Chao Phraya River basin, Thailand, Using the MRI-GCM3.1S Dataset. *Journal of the Meteorological Society of Japan*, 90(2), 137–150.
- Kure, S., & Tebakari, T. (2012). Hydrological impact of regional climate change in the Chao Phraya River Basin, Thailand. *Hydrological Research Letters*, 6(0), 53–58. <https://doi.org/10.3178/hrl.6.53>
- Lara, A., Villalba, R., & Urrutia, R. (2008). A 400-year tree-ring record of the Puelo River summer–fall streamflow in the Valdivian Rainforest eco-region, Chile. *Climatic Change*, 86(3–4), 331–356. <https://doi.org/10.1007/s10584-007-9287-7>
- Li, J., Xie, S., Cook, E., & Morales, M. (2013). El Niño modulations over the past seven centuries. *Nature Climate Change*, 3(9), 822–826. <https://doi.org/10.1038/nclimate1936>
- Li, R., Wang, S., Gillies, R., Buckley, B. M., Yoon, J.-H., & Cho, C. (2018). Regional trends in early-monsoon rainfall over Vietnam and CCSM4 attribution. *Climate Dynamics*, 52(1–2), 363–372. <https://doi.org/10.1007/s00382-018-4198-z>
- Liu, X., An, W., Treydte, K., Shao, X., Leavitt, S., Hou, S., et al. (2011). Tree-ring  $\delta^{18}\text{O}$  in southwestern China linked to variations in regional cloud cover and tropical sea surface temperature. *Chemical Geology*, 291, 104–115.
- Liu, Y., Cobb, K., Song, H., Li, Q., Li, C., & Nakatsuka, T. (2017). Recent enhancement of central Pacific El Niño variability relative to last eight centuries. *Nature Communications*, 8, 15386. <https://doi.org/10.1038/ncomms15386>
- MacDonald, G., & Case, R. (2005). Variations in the Pacific Decadal Oscillation over the past millennium. *Geophysical Research Letters*, 32, L08703. <https://doi.org/10.1029/2005GL022478>
- Mann, M., & Lees, J. (1996). Robust estimation of background noise and signal detection in climatic time series. *Climatic Change*, 33(3), 409–445. <https://doi.org/10.1007/BF00142586>
- Mantua, N., Hare, S., Zhang, Y., Wallace, J., & Francis, R. (1997). A Pacific interdecadal climate oscillation with impacts on salmon production. *Bulletin of the American Meteorological Society*, 78(6), 1069–1079. [https://doi.org/10.1175/1520-0477\(1997\)078<1069:APICOW>2.0.CO;2](https://doi.org/10.1175/1520-0477(1997)078<1069:APICOW>2.0.CO;2)
- McGregor, S., Timmermann, A., & Timm, O. (2010). A unified proxy for ENSO and PDO variability since 1650. *Climate of the Past*, 6(1), 1–17. <https://doi.org/10.5194/cp-6-1-2010>
- Meehl, G., Hu, A., Arblaster, J. M., Fasullo, J., & Trenberth, K. (2013). Externally forced and internally generated decadal climate variability associated with the Interdecadal Pacific Oscillation. *Journal of Climate*, 26(18), 7298–7310. <https://doi.org/10.1175/JCLI-D-12-00548.1>
- Meko, D., Woodhouse, C., & Morino, K. (2012). Dendrochronology and links to streamflow. *Journal of Hydrology*, 412–413(1), 200–209. <https://doi.org/10.1016/j.jhydrol.2010.11.041>
- Nguyen, H., & Galelli, S. (2017). A linear dynamical systems approach to streamflow reconstruction reveals history of regime shifts in northern Thailand. *Water Resources Research*, 54, 2057–2077. <https://doi.org/10.1002/2017WR022114>
- Promchote, P., Wang, S., & Johnson, P. (2016). The 2011 Great flood in Thailand: Climate diagnostics and implications from climate change. *Journal of Climate*, 29(1), 367–379.
- Pumijumnon, N., & Eckstein, D. (2011). Reconstruction of pre-monsoon weather conditions in northwestern Thailand from the tree-ring widths of *Pinus merkusii* and *Pinus kesiya*. *Trees*, 25(1), 125–132. <https://doi.org/10.1007/s00468-010-0528-4>
- Re, S. (2011). Natural catastrophes and man-made disasters in 2011. *Sigma*, (1).
- Risi, C., Bony, S., & Vimeux, F. (2008). Influence of convective processes on the isotopic composition ( $\text{d}^{18}\text{O}$  and  $\text{dD}$ ) of precipitation and water vapor in the tropics: 2. Physical interpretation of the amount effect. *Journal of Geophysical Research*, 113, D19306. <https://doi.org/10.1029/2008JD009943>
- Roy, S., Goodrich, G., & Balling, R. (2003). Influence of El Niño/Southern Oscillation, Pacific decadal oscillation, and local sea-surface temperature anomalies on peak season monsoon precipitation in India. *Climate Research*, 25(25), 171–178. <https://doi.org/10.3354/cr025171>
- Saji, N., Goswami, B., Vinayachandran, P., & Yamagata, T. (1999). A dipole mode in the tropical Indian Ocean. *Nature*, 401(6751), 360–363. <https://doi.org/10.1038/43854>
- Sano, M., Xu, C., & Nakatsuka, T. (2012). A 300-year Vietnam hydroclimate and ENSO variability record reconstructed from tree ring  $\delta^{18}\text{O}$ . *Journal of Geophysical Research*, 117, D12115. <https://doi.org/10.1029/2012JD017749>
- Sen Roy, S., & Sen Roy, N. (2011). Influence of Pacific Decadal Oscillation and El Niño–Southern Oscillation on the summer monsoon precipitation in Myanmar. *International Journal of Climatology*, 31(1), 14–21. <https://doi.org/10.1002/joc.2065>
- Shen, C., Wang, W.-C., Gong, W., & Hao, Z. (2006). A Pacific Decadal Oscillation record since 1470 AD reconstructed from proxy data of summer rainfall over eastern China. *Geophysical Research Letters*, 33, L03702. <https://doi.org/10.1029/2005GL024804>
- Singhratna, N., Rajagopalan, B., Kumar, K. K., & Clark, M. (2005). Interannual and interdecadal variability of Thailand summer monsoon season. *Journal of Climate*, 18(11), 1697–1708.
- Siripong, H., Wirat, K., & Suwit, T. (2000). Flood management in Chao Phraya River basin, The Chao Phraya Delta: Historical development, dynamics and challenges of Thailand's rice bowl. Proceeding of the International Conference, 12–15 December 2000, Kasetsart University, Bangkok, Thailand.
- Stockton, C., & Jacoby, G. (1976). Long-term surface water supply and streamflow levels in the Upper Colorado River Basin. In *Lake Powell Research Project, Bulletin* (Vol. 18, pp. 1–70). Los Angeles, California: Institute of Geophysics and Planetary Physics, University of California.
- Stuecker, M. F. (2018). Revisiting the Pacific meridional mode. *Scientific Reports*, 8(1), 1–9. <https://doi.org/10.1038/s41598-018-21537-0>
- Tierney, J., Abram, N., Anchukaitis, K., Evans, M., Cyril, G., Halimeda, K., et al. (2015). Tropical sea-surface temperatures for the past four centuries reconstructed from coral archives. *Paleoceanography*, 30, 226–252. <https://doi.org/10.1002/2014PA002717>
- Torrence, C., & Webster, P. (1999). Interdecadal changes in the ENSO–monsoon system. *Journal of Climate*, 12(8), 2679–2690. [https://doi.org/10.1175/1520-0442\(1999\)012<2679:ICITEM>2.0.CO;2](https://doi.org/10.1175/1520-0442(1999)012<2679:ICITEM>2.0.CO;2)

- Wang, S., Huang, J., He, Y., & Guan, Y. (2014). El Niño-Southern Oscillation on global land dry-wet changes. *Scientific Reports*, 4(1), 6651. <https://doi.org/10.1038/srep06651>
- Woodhouse, C., Gray, S., & Meko, D. (2006). Updated streamflow reconstructions for the Upper Colorado River Basin. *Water Resources Research*, 42, W05415. <https://doi.org/10.1029/2005WR004455>
- Xu, C., Ge, J., Nakatsuka, T., Yi, L., Zheng, H., & Sano, M. (2016). Potential utility of tree ring  $\delta^{18}\text{O}$  series for reconstructing precipitation records from the lower reaches of the Yangtze River, southeast China. *Journal of Geophysical Research: Atmospheres*, 121, 3954–3968. <https://doi.org/10.1002/2015JD023610>
- Xu, C., Pumijumnong, N., Nakatsuka, T., Sano, M., & Guo, Z. (2018). Inter-annual and multi-decadal variability of monsoon season rainfall in central Thailand during the period 1804–1999, as inferred from tree ring oxygen isotopes. *International Journal of Climatology*, 38(15), 5766–5776. <https://doi.org/10.1002/joc.5859>
- Xu, C., Pumijumnong, N., Nakatsuka, T., Sano, M., & Li, Z. (2015). A tree-ring cellulose  $\delta^{18}\text{O}$ -based July–October precipitation reconstruction since AD 1828, northwest Thailand. *Journal of Hydrology*, 529, 433–441. <https://doi.org/10.1016/j.jhydrol.2015.02.037>
- Xu, C., Sano, M., & Nakatsuka, T. (2011). Tree ring cellulose  $\delta^{18}\text{O}$  of *Fokienia hodginsii* in northern Laos: A promising proxy to reconstruct ENSO? *Journal of Geophysical Research*, 116, D24109. <https://doi.org/10.1029/2011JD016694>
- Xu, C., Sano, M., & Nakatsuka, T. (2013). A 400-year record of hydroclimate variability and local ENSO history in northern Southeast Asia inferred from tree-ring  $\delta^{18}\text{O}$ . *Palaeogeography, Palaeoclimatology, Palaeoecology*, 386, 588–598. <https://doi.org/10.1016/j.palaeo.2013.06.025>
- Xu, C., Shi, J., Zhao, Y., Nakatsuka, T., Sano, M., Shi, S., & Guo, Z. (2018). Early summer precipitation in the lower Yangtze River basin for AD 1845–2011 based on tree-ring cellulose oxygen isotopes. *Climate Dynamics*, 52(3–4), 1583–1594. <https://doi.org/10.1007/s00382-018-4212-5>
- Xu, C., Zheng, H., Nakatsuka, T., & Sano, M. (2013). Oxygen isotope signatures preserved in tree ring cellulose as a proxy for April–September precipitation in Fujian, the subtropical region of southeast China. *Journal of Geophysical Research: Atmospheres*, 118, 12,805–12,815. <https://doi.org/10.1002/2013JD019803>
- Yoon, J. H., Wang, S. S., Gillies, R. R., Kravitz, B., Hipps, L., & Rasch, P. (2015). Increasing water cycle extremes in California and in relation to ENSO cycle under global warming. *Nature Communications*, 6(1), 8657. <https://doi.org/10.1038/ncomms9657>
- Yu, J., Kao, H., & Lee, T. (2010). Subtropics-related interannual sea surface temperature variability in the equatorial central Pacific. *Journal of Climate*, 23(11), 2869–2884. <https://doi.org/10.1175/2010JCLI3171.1>
- Yu, J., Lu, M., & Kim, S. (2012). A change in the relationship between tropical central Pacific SST variability and the extratropical atmosphere around 1990. *Environmental Research Letters*, 7(3), 034025. <https://doi.org/10.1088/1748-9326/7/3/034025>
- Zhang, L., & Delworth, T. (2015). Analysis of the characteristics and mechanisms of the Pacific Decadal Oscillation in a suite of coupled models from the Geophysical Fluid Dynamics Laboratory. *Journal of Climate*, 28(19), 7678–7701. <https://doi.org/10.1175/JCLI-D-14-00647.1>
- Zhu, M., Stott, L., Buckley, B. M., & Yoshimura, K. (2012). 20th century seasonal moisture balance in Southeast Asian montane forests from tree cellulose  $\delta^{18}\text{O}$ . *Climatic Change*, 115(3–4), 505–517. <https://doi.org/10.1007/s10584-012-0439-z>
- Zhu, M., Stott, L., Buckley, B. M., Yoshimura, K., & Ra, K. (2012). Indo-Pacific Warm Pool convection and ENSO since 1867 AD derived from Cambodian pine tree cellulose oxygen isotopes. *Journal of Geophysical Research*, 117, D11307. <https://doi.org/10.1029/2011JD017198>